Research Article | Vol. 26, No. 15 | 23 Jul 2018 | OPTICS EXPRESS 19445
Optics EXPRESS

Bimodal grating coupler design on SOI technology for mode division multiplexing at 1550 nm

DAVID GARCIA-RODRIGUEZ,* JUAN L. CORRAL, AMADEU GRIOL, AND ROBERTO LLORENTE

Nanophotonics Technology Centre, Universitat Politècnica de València, Camino de Vera s/n, 46022 Valencia, Spain
**dgarciarodriguez@ntc.upv.es*

Abstract: In this paper, we evaluate by means of simulation and experimentally the simultaneous coupling of the LP_{01x}-LP_{11ax} fiber modes and the TE_0-TE_1 nanophotonic SOI waveguide modes using a grating coupler for a two-mode fiber at 1550 nm. Both the grating width (ranging from 10 µm to 15 µm) and the grating vertical profile have been considered in the design procedure. The optimum design (14 µm width and 609 nm grating period) has been selected in terms of coupling efficiency (both LP_{01x}-TE_0 and LP_{11ax}-TE_1), compactness and tolerance to lateral misalignments between fiber and coupler. The LP_{01x}-TE_0 and LP_{11ax}-TE_1 modes achieved coupling efficiencies of 49% and 45%, respectively.

OCIS codes: (050.2770) Gratings; (060.1810) Buffers, couplers, routers, switches, and multiplexers; (060.4230) Multiplexing; (130.3120) Integrated optics devices; (230.7400) Waveguides, slab.

References and links

1. D. J. Richardson, "New optical fibres for high-capacity optical communications," Philos Trans A Math Phys Eng Sci **374**(2062), 20140441 (2016).
2. M. Kasahara, K. Saitoh, T. Sakamoto, N. Hanzawa, T. Matsui, K. Tsujikawa, F. Yamamoto, and M. Koshiba, "Design of few-mode fibers for mode-division multiplexing transmission," IEEE Photonics J. **5**(6), 7201207 (2013).
3. H. Chen, V. Sleiffer, B. Snyder, M. Kuschnerov, R. Uden, Y. Jung, C. M. Okonkwo, O. Raz, P. O'Brien, H. Waardt, and T. Koonen, "Demonstration of a photonic integrated mode coupler with MDM and WDM transmission," IEEE Photonics Technol. Lett. **25**(21), 2039–2042 (2013).
4. C. Sun, Y. Yu, M. Ye, G. Chen, and X. Zhang, "An ultra-low crosstalk and broadband two-mode (de)multiplexer based on adiabatic couplers," Sci. Rep. **6**(1), 38494 (2016).
5. J. Xing, Z. Li, X. Xiao, J. Yu, and Y. Yu, "Two-mode multiplexer and demultiplexer based on adiabatic couplers," Opt. Lett. **38**(17), 3468–3470 (2013).
6. D. Garcia-Rodriguez, J. L. Corral, A. Griol, and R. Llorente, "Dimensional variation tolerant mode converter/multiplexer fabricated in SOI technology for two-mode transmission at 1550 nm," Opt. Lett. **42**(7), 1221–1224 (2017).
7. D. Garcia-Rodriguez, J. L. Corral, and R. Llorente, "Mode Conversion for Mode Division Multiplexing at 850 nm in Standard SMF," IEEE Photonics Technol. Lett. **29**(11), 929–932 (2017).
8. Z. Zhang, X. Hu, and J. Wang, "On-chip optical mode exchange using tapered directional coupler," Sci. Rep. **5**(1), 16072 (2015).
9. Y. Ding, J. Xu, F. Da Ros, B. Huang, H. Ou, and C. Peucheret, "On-chip two-mode division multiplexing using tapered directional coupler-based mode multiplexer and demultiplexer," Opt. Express **21**(8), 10376–10382 (2013).
10. A. Zanzi, A. Brimont, A. Griol, P. Sanchis, and J. Marti, "Compact and low-loss asymmetrical multimode interference splitter for power monitoring applications," Opt. Lett. **41**(2), 227–229 (2016).
11. T. Uematsu, K. Saitoh, N. Hanzawa, T. Sakamoto, T. Matsui, K. Tsujikawa, and M. Koshiba, "Low-loss and broadband PLC-type mode (de)multiplexer for mode-division multiplexing transmission," in *OFC2013* (2013), paper OTh1B.5 (2013).
12. N. Hanzawa, K. Saitoh, T. Sakamoto, T. Matsui, K. Tsujikawa, M. Koshiba, and F. Yamamoto, "Two-mode PLC-based mode multi/demultiplexer for mode and wavelength division multiplexed transmission," Opt. Express **21**(22), 25752–25760 (2013).
13. Y. Lai, Y. Yu, S. Fu, J. Xu, P. P. Shum, and X. Zhang, "Efficient spot size converter for higher-order mode fiber-chip coupling," Opt. Lett. **42**(18), 3702–3705 (2017).

#327722 https://doi.org/10.1364/OE.26.019445
Journal © 2018 Received 13 Apr 2018; revised 1 Jun 2018; accepted 2 Jun 2018; published 18 Jul 2018

Optics EXPRESS

14. N. Hatori, T. Shimizu, M. Okano, M. Ishizaka, T. Yamamoto, Y. Urino, M. Mori, T. Nakamura, and Y. Arakawa, "A Hybrid Integrated Light Source on a Silicon Platform Using a Trident Spot-Size Converter," J. Lightwave Technol. **32**(7), 1329–1336 (2014).
15. N. Hanzawa, K. Saitoh, T. Sakamoto, T. Matsui, K. Tsujikawa, M. Koshiba, and F. Yamamoto, "Mode multi/demultiplexing with parallel waveguide for mode division multiplexed transmission," Opt. Express **22**(24), 29321–29330 (2014).
16. D. Dai and M. Mao, "Mode converter based on an inverse taper for multimode silicon nanophotonic integrated circuits," Opt. Express **23**(22), 28376–28388 (2015).
17. D. Taillaert, F. Van Laere, M. Ayre, W. Bogaerts, D. Van Thourhout, P. Bienstman, and R. Baets, "Grating Couplers for Coupling between Optical Fibers and Nanophotonic Waveguides," Jpn. J. Appl. Phys. **45**(8A), 6071–6077 (2006).
18. S. Lardenois, D. Pascal, L. Vivien, E. Cassan, S. Laval, R. Orobtchouk, M. Heitzmann, N. Bouzaida, and L. Mollard, "Low-loss submicrometer silicon-on-insulator rib waveguides and corner mirrors," Opt. Lett. **28**(13), 1150–1152 (2003).
19. R. Orobtchouk, A. Layadi, H. Gualous, D. Pascal, A. Koster, and S. Laval, "High-efficiency light coupling in a submicrometric silicon-on-insulator waveguide," Appl. Opt. **39**(31), 5773–5777 (2000).
20. Y. Ding, H. Ou, J. Xu, M. Xiong, and C. Peucheret, "On-chip mode multiplexer based on a single grating coupler" in *IEEE Photonics Conference IPC* (IEEE, 2012), paper ThB4.
21. B. Wohlfeil, G. Rademacher, C. Stamatiadis, K. Voigt, L. Zimmermann, and K. Petermann, "A Two-Dimensional Fiber Grating Coupler on SOI for Mode Division Multiplexing," IEEE Photonics Technol. Lett. **28**(11), 1241–1244 (2016).
22. A. M. J. Koonen, H. Chen, H. P. A. van den Boom, and O. Raz, "Silicon photonic integrated mode multiplexer and demultiplexer," IEEE Photonics Technol. Lett. **24**(21), 1961–1964 (2012).
23. Y. Ding, H. Ou, J. Xu, and C. Peucheret, "Silicon photonic integrated circuit mode multiplexer," IEEE Photonics Technol. Lett. **25**(7), 648–651 (2013).
24. J. V. Galan, P. Sanchis, J. Blasco, and J. Marti, "Study of High Efficiency Grating Couplers for Silicon-Based Horizontal Slot Waveguides," IEEE Photonics Technol. Lett. **20**(12), 985–987 (2008).
25. G. Roelkens, D. Van Thourhout, and R. Baets, "High efficiency Silicon-on-Insulator grating coupler based on a poly-Silicon overlay," Opt. Express **14**(24), 11622–11630 (2006).
26. D. Taillaert, "Grating couplers as Interface between Optical Fibres and Nanophotonic Waveguides," PhD Dissertation, Universiteit Gent, 2005.

1. Introduction

In the last decade, the data traffic demand has been continuously increasing due to new internet based-services, particularly video streaming and machine-to-machine communications, driving optical-communication systems based on single-mode fibers to their capacity limit [1]. Spatial-division multiplexing (SDM) or mode-division multiplexing (MDM) are promising techniques to overcome the capacity limit of the optical fiber [1]. In its simplest implementation, MDM permits to propagate the LP_{01} and LP_{11} modes in a two-mode fiber (TMF) [2].

Silicon-on-insulator (SOI) or planar lightwave circuit (PLC) are key technologies to provide low-cost photonic integrated mode converters and mode (de)multiplexers. Different techniques have been proposed to convert and (de)multiplex the modes; for example, asymmetrical directional couplers (ADC), multimode interference (MMI), tapered directional coupler, adiabatic couplers, inverse tapers or trident couplers [3–14].

An important aspect in the different integrated devices for MDM is the coupling to the optical fiber. Depending on the employed technology, a vertical or horizontal coupling is required. On one hand, PLC favors the use of the horizontal coupling due to the similar dimensions between the waveguide and the fiber core. This technology offers low loss and mass productivity due to their mature manufacturing technology. However, the main drawback are the higher sizes and higher bending radius (above 5 cm [15]). On the other hand, SOI technology offers lower size, better repeatability and higher robustness than the PLC based devices but the coupling to the fiber is more demanding.

When a few mode fiber (FMF) is under consideration the coupling of the different modes to/from the SOI waveguides must be solved. SOI with horizontal coupling are traditional based on spot size converter which were limited to the fiber fundamental mode [13]. Recently some modifications have been proposed in order to combine several inverse taper spot size converters by means of Y-junction or trident waveguides to couple to fiber higher modes [13,

Optics EXPRESS

14]. The inverse tapers provide highly efficient, polarization insensitive, and broad bandwidth optical coupling but they require a high alignment precision, a complex design and long lengths [13, 16]. Besides, a single horizontal coupler is required for each fiber mode to couple.

On the other hand, vertical coupling in SOI technology is based on the use of grating couplers. Grating couplers have been successfully used to couple the TE_0 mode of the SOI waveguide to the LP_{01} mode of the standard single mode fiber (SSMF), and vice versa [17–19]. Although grating couplers are easy to fabricate and provide on chip test measurements with small footprints, the main drawbacks are the limited bandwidth and their polarization sensitivity.

One first approach to vertically couple light from the SOI waveguide to the LP_{01}/LP_{11} modes in a FMF was based on the use of one 2D grating coupler excited from two 90 degrees apart waveguides propagating the TE_0 and TE_1 modes [20]. Other proposed SOI devices are based on the use of 2D gratings simultaneously excited from several waveguides propagating the TE_0 modes but with a fixed phase relation between the waveguide modes [21–23]. These devices offer the generation of up to six fiber modes (all LP_{01} and LP_{11} degenerated modes) but a more complex feeder circuit is required with a higher footprint and thermal tuning to adjust the phase shift at the different waveguides [21–23]. A strictly vertical coupling to the fiber is also required on these devices with the corresponding issues of second order reflection at the waveguide fiber interface [20–23].

Thus, using a single grating coupler that couples simultaneously the TE_0 and TE_1 modes from a single SOI waveguide to the LP_{01} and LP_{11} modes in the FMF would be a key component for low cost and low size integrated devices in the MDM systems.

In this letter, a grating coupler for the simultaneous coupling of the TE_0 and TE_1 modes into one single polarization of the LP_{01} mode and one single polarization and azimuthal orientation of the LP_{11} mode of the TMF is designed. Both the nominal performance of the grating coupler at the design wavelength and the sensibility of the coupling efficiency to lateral misalignment of the fiber are considered. The best grating design is selected in terms of both TE_0-LP_{01} and TE_1-LP_{11} coupling. The selected device has been fabricated and measured.

2. Grating coupler design

The general concept of the MDM link is depicted in Fig. 1. It consists of two lasers emitting at 1550 nm propagating the LP_{01} mode in a standard single-mode fiber (SSMF). Both LP_{01} modes pass through a polarization controller to impinge the standard LP_{01}-TE_0 grating coupler with the s-polarization. The TE_0 mode from the upper branch is converted into the TE_1 mode and it is multiplexed with the optical signal coming from the lower branch, propagating both modes, TE_0 and TE_1, to the common output. The TE_1 mode is excited and coupled to the TMF propagating the LP_{11a} mode with s-polarization. Finally, both modes are coupled to the two mode fiber (TMF) using a specific grating coupler, corresponding now to the fiber LP_{01} and LP_{11a} modes. At the receiver, the same device is used in order to demultiplex each mode to the corresponding photodiode. As in any other mode demultiplexer based on vertical grating couplers, the polarization of the fiber modes must be properly aligned to the s-polarization at the fiber waveguide interface. Depending on the mode coupling induced by the TMF link a multiple input multiple output (MIMO) digital processing stage could be required at the receiver to properly split both data streams.

Optics EXPRESS

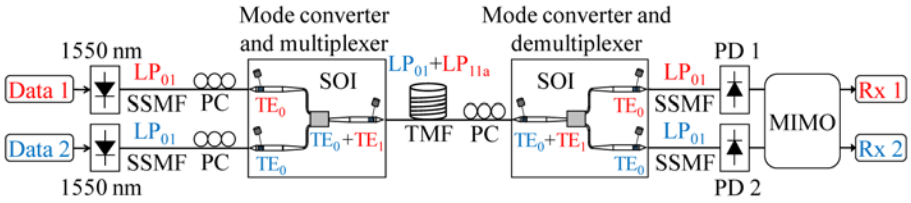

Fig. 1. Scheme for mode-division multiplexing (MDM) at 1550 nm with two-mode fiber (TMF) optical transmission media.

2.1 Grating theory

The periodic structures are defined by the Bragg condition that describes the relation between the wave-vectors of the incident and diffracted waves. In the case of waveguide grating couplers, the incident wave is replaced by the guided mode of the waveguide, which is characterized by its propagation constant β. The equation can be defined as [24]

$$\frac{2\pi}{\lambda} n_{cover} \sin(\theta_m) = \frac{2\pi}{\lambda} n_{eff} + m\frac{2\pi}{\Lambda} \tag{1}$$

where λ is the design wavelength, n_{cover} is the refractive index of the cover substrate, θ_m is the tilt angle, n_{eff} the effective index of the optical mode in the grating waveguide, Λ is the grating period and the integer m is the diffraction order.

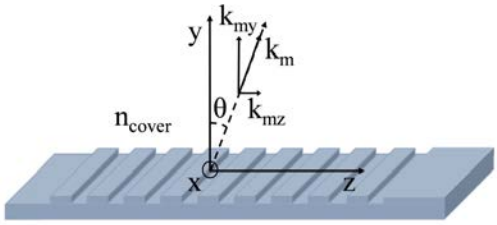

Fig. 2. Schematic waveguide grating coupler diagram for coupling light to/from an optical fiber.

Considering the grating as an output coupler, the coupling to the optical fiber is done for the first diffraction order ($m = -1$) with a specific tilted angle (θ), as depicted in Fig. 2. In the case of simultaneous TE_0 and TE_1 modes coupling, Eq. (1) must be fulfilled in both cases, therefore, the effective indexes for both modes need to be approximately equal. If the waveguide widths are sufficiently large, the TE_0 and TE_1 modes are expected to have similar effective indexes.

The coupling efficiency from fiber to waveguide is the same as from waveguide to fiber due to reciprocity theorem. When the electromagnetic fields at the position of the fiber facet are known, the coupling efficiency to fiber becomes [25]

$$\eta = \left| \iint_S E \times H_{fib}^{*} dS \right|^2 \tag{2}$$

where E is the normalized electrical field of the diffracted wave from the grating, and H_{fib} is the normalized magnetic fields of the optical mode in the fiber and S is the fiber facet. Equation (2) is a good approximation, even if the grating is covered by air instead of silica [26].

When the optical mode of the waveguide is launched from the grating, some light is refracted upwards and the rest is refracted downwards (across the substrate), due to the vertical grating symmetry. Thus, for this design the efficiency will not be higher than 50% unless reflective elements are used [17, 24].

Optics EXPRESS

The complete coupler problem is a 3D problem but can be approximated by two 2D problem due to the highly different dimensions between the waveguide width and height where the width is much larger than the height. In Fig. 3, the fundamental mode (TE_0) and the first higher order mode (TE_1) for a 12 µm SOI waveguide width are shown.

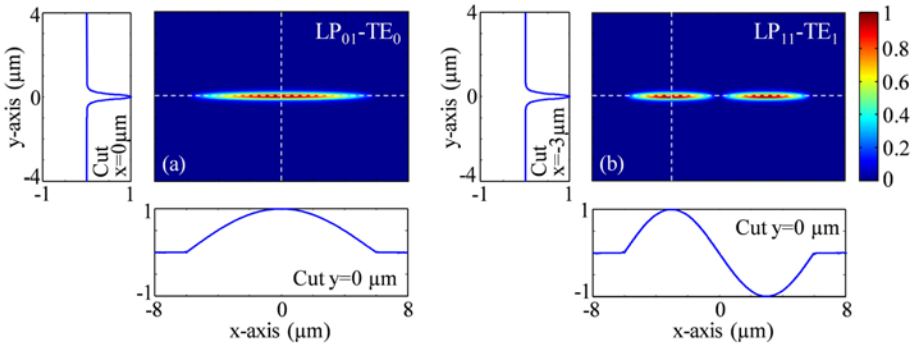

Fig. 3. 2D Near-field pattern and 1D x-y cuts for the TE_0 and TE_1 modes considering a 12 µm wide and 220 nm high SOI waveguide. (a) TE_0 mode with x = 0 µm and y = 0 µm cuts, (b) TE_1 mode with x = –3 µm and y = 0 µm cuts.

2.2 Grating design

As previously commented, the complete coupler design problem can be divided into two 2D problems. Firstly we will assess the width of the grating coupler by taking into account the overlap between the mode field distributions in the transverse planes of both the SOI waveguide and the FMF. The most common grating coupler design based on SOI technology (SiO_2 layer height = 220 nm) for the TE_0-LP_{01} coupling to SMF-28 fiber has a waveguide width (w_g) of 12 µm [17]. If we take a TMF at 1550 nm such as SM2000 fiber from Thorlabs (11 µm core diameter with a SiO_2 cladding, n_{core} = 1.4495 at 1550 nm), the LP_{01} mode profile is slightly wider than the LP_{01} mode profile for the SMF-28 (11 µm in SM2000 vs. 10.4 µm in SMF-28). Besides, the TE_1 mode needs to be coupled to the LP_{11} mode and, as shown in Fig. 4, the LP_{11} mode profile in the SM2000 fiber is much wider than the TE_1 mode profile in the 12 µm waveguide. If the peak of the modes are taken as a reference, the LP_{11} mode is 1.64 µm wider than the TE_1 mode. Therefore, the optimum waveguide width is expected to be 1 µm to 2 µm greater than 12 µm.

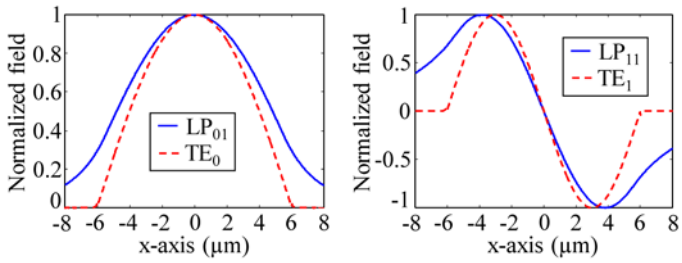

Fig. 4. Comparison between the normalized horizontal field profile of the LP_{01} and LP_{11} modes from SM2000 fiber and the TE_0 and TE_1 modes for a SOI waveguide (height = 220 nm and waveguide width = 12 µm).

The grating coupler is composed by a Si core (t_{core}), a SiO_2 cladding ($t_{cladding}$) and a Si substrate ($t_{substrate}$), as can be seen in Fig. 5. We use SOI wafers of 220 nm/2 µm Si/SiO_2 layers thicknesses, corresponding to t_{core} and $t_{cladding}$. The upper cladding layer of the grating is supposed to be air. The main parameters in the grating coupler design are the filling factor or duty cycle ($ff = w/\Lambda$), the grating period (Λ) and the etching depth (e_d). Some typical values

Optics EXPRESS

for the TE_0-LP_{01} coupling using SMF-28 are: ff = 0.5, e_d = 70 nm and Λ = 630 nm, to maximize coupling efficiency at 1550 nm [26]. The incident angle (Θ) is around 10 degrees in order to optimize the coupling efficiency and avoid reflections.

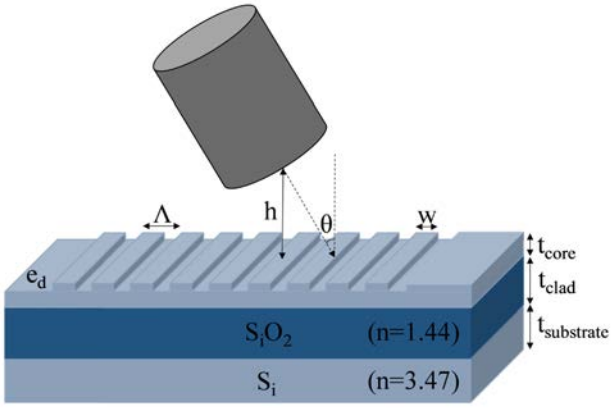

Fig. 5. Grating coupler scheme based on SOI technology with an input fiber.

Figure 6 shows the simulation results of the coupling efficiency for the LP_{01}-TE_0 and LP_{11}-TE_1 modes with respect to the grating period and the filling factor. The results shown in this figure have been obtained according to the simulation approach described in section 3 for a 12 µm waveguide width. Figure 6(a) results show a maximum efficiency region corresponding to an almost vertical line with optimum grating periods ranging from 607 nm to 611 nm when the filling factor varies from 0.48 to 0.52, respectively. From all these possible design parameters the optimum grating period, Λ = 609 nm, for a filling factor of ff = 0.5 was selected. A similar performance is shown in Fig. 6(b) for the TE_1-LP_{11} coupling. Figure 6 was also simulated for different grating widths (w_g = 10 to 15 µm) with no influence on the results shown for w_g = 12 µm. Once the filling factor and the grating period were fixed the sensitivity to variations of the etching depth was found to be of less magnitude than the tolerance of the fabrication process in the vertical dimension so the typical 70 nm etching depth was not modified.

Finally, it can be stated that both couplings (TE_0-LP_{01}, TE_1-LP_{11}) obtained the maximum efficiency for the same design parameters of the grating coupler and, therefore, it is possible to couple them simultaneously.

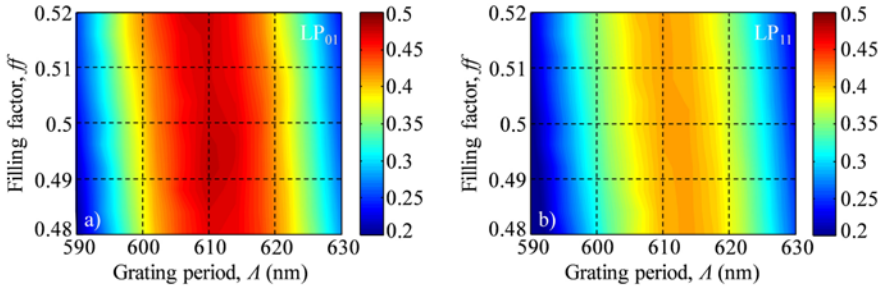

Fig. 6. Coupling efficiency as a function of the grating period and filling factor for: (a) LP_{01}-TE_0 modes and (b) LP_{11}-TE1 modes coupling.

Once the vertical dimensions of the grating coupler are fixed (t_{core} = 220 nm, e_d = 70 nm, ff = 0.5) the SOI mode indexes in the grating can be estimated as the average value between the effective indexes of the unperturbed (t_{core} = 220 nm) and perturbed (t_{core}-e_d = 150 nm) waveguides. For a w_g = 12 µm grating width quite similar effective indexes (n_{effTE0} = 2.6920

Optics EXPRESS

vs n_{effTE1} = 2.6897) are obtained. As aforementioned in the grating theory subsection, both modes effective indexes are quite similar so Eq. (1) is fulfilled simultaneously and the small index difference would translate to a negligible 0.13 degrees difference in the incident angle. Thus, the grating coupler can be used for simultaneous coupling.

3. Simulation

Simulations of fiber-grating coupling has been performed using 3D Finite Difference Time Domain method (3D-FDTD). Eigenmodes' effective indices in waveguides and optical fibers are obtained by means of three-dimensional (3D) finite element method (3D-FEM) and three-dimensional beam (3D) propagation method (3D-BPM), respectively.

FDTD method is appropriate to simulate reduced regions with fast speed and low memory requirements. Therefore, we optimize the fiber height above the grating (h = 1 μm) to reduce our simulation region. Complete grating coupler has been simulated at 1550 nm for different waveguide widths (10 μm, 11 μm, 12 μm, 13 μm, 14 μm and 15 μm). The refractive indexes of Si and SiO_2 are taken as n_{Si} = 3.4758 and n_{SiO2} = 1.4442, respectively. LP_{01} and LP_{11} modes are excited from the optical fiber and coupled to the waveguide. In order to assess the sensitivity to eventual fiber to coupler misalignments, the center of the fiber can be displaced along the width of the grating from −4 μm to 4 μm with respect to the center of the grating coupler. Results of the coupling efficiency are depicted in Fig. 7.

Figure 7(a) displays the coupling efficiency (CE) from LP_{01} to TE_0 and the undesired coupling efficiency from LP_{01} to TE_1, or leakage, as a function of displacement. All coupling efficiencies are symmetric and slow-varying with respect to the center of the grating coupler, remaining practically constant for minor variations (up to ± 1 μm). However, depending on the selected width, the coupling efficiency from LP_{01} to TE_0 increases from 26.4% (for a shift of 4 μm) to as high as 45.9% (no misplacement) for the 10 μm width or, from 29.3% to as high as 49.7%, respectively, for the 15 μm width. For the maximum coupling, the difference between both grating widths is 3.8%. If a 1 dB penalty in the coupling efficiency due to lateral misplacement is considered a ± 2.4 μm (10 μm coupler) to ± 2.6 μm (15 μm coupler) alignment range are obtained. Besides that, the LP_{01} to TE_1 leakage is null for all widths when the fiber and the grating are perfectly aligned, but it ranges from 8.4% (w_g = 15 μm) to 13.3% (w_g = 10 μm) for the maximum misplacement considered. The best performance in terms of LP_{01} to TE_0 coupling efficiency is obtained for w_g = 15 μm with a 49.7% efficiency, value that would decrease for wider widths (49.6% and 49.1% for w_g = 16 μm and w_g = 17 μm). With this result in mind, widths wider than 15 μm were not taken into consideration in the simulation.

The simulation results for the coupling efficiency from LP_{11} to TE_1 and the undesired LP_{11} to TE_0 leakage are shown in Fig. 7(b). In this case, the different responses are also symmetric with respect to the center of the grating coupler, but the sensitivity to lateral misalignment is quite higher than in the LP_{01}-TE_0 case. From LP_{11} to TE_1, the coupling efficiency increases approximately from 0.2% (for a lateral displacement of 4 μm) to 34.8% (no misplacement) for the 10 μm width or, from 3.5% to as high as 46.35%, respectively, for the 15 μm width. In this case, the maximum difference between both cases is 11.5%, 3 times higher than for the LP_{01}-TE_0 coupling. The alignment range for the same 1 dB coupling efficiency penalty is reduced to ± 1.25 μm (10 μm coupler) to ± 1.35 μm (15 μm coupler) in this case. In terms of LP_{11} to TE_0 leakage, the efficiency at the maximum misplacement ranges from 42.3% to 21.8% for the 10 μm and 15 μm widths, respectively. It can be stated that LP_{11} shows a remarkable dependence with the waveguide width and the lateral displacement.

Even though the coupling efficiency simulation results imply that the w_g = 15 μm, Λ = 609 nm, ff = 0.5, e_d = 70 nm grating coupler would be the best option in terms of coupling efficiency a w_g = 14 μm width has been selected to be fabricated as the best compromise when the integrated device size is also considered. The improvement in coupling efficiency with the wider coupler (0.1% and 1.2% difference for LP_{01}-TE_0 and LP_{11}-TE_1 coupling,

Optics EXPRESS

respectively) is incremental and the increase of 1 μm in width (9.3% increase) would translate to a quite longer adiabatic taper, increasing the device footprint by the same 9.3% factor. It is important to point out that the final design is 2 μm wider than the optimum design for the LP_{01}-TE_0 and SMF-28 fiber, according to the SOI state-of-art. In this conventional LP_{01}-TE_0 grating coupler design for SMF-28 fiber the selected width (w_g = 12 μm) is also slightly narrower than the optimal theoretical width.

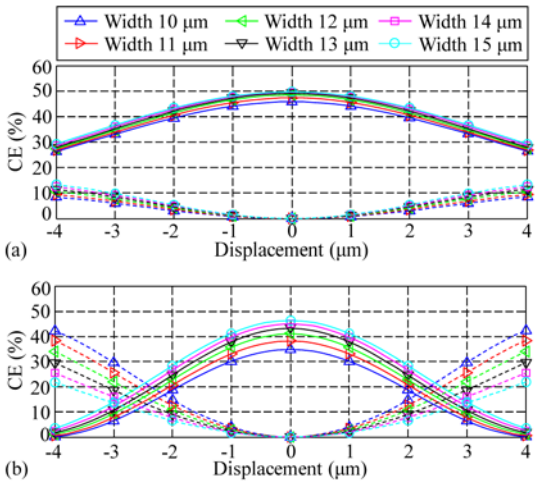

Fig. 7. (a) Coupling efficiency from LP_{01} to TE_0 (solid line) and from LP_{01} to TE_1 (dashed line) and (b) Coupling efficiency from LP_{11} to TE_1 (solid line) and from LP_{11} to TE_0 (dashed line).

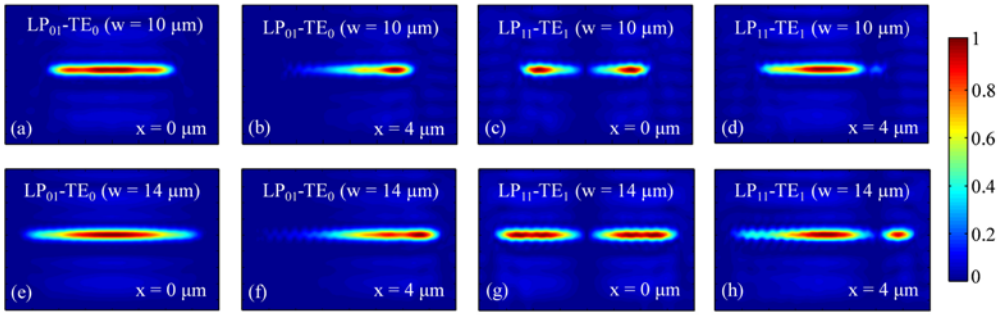

Fig. 8. Normalized optical intensity in the SOI waveguide (width w_g, height 220 nm) when the grating coupler is excited from a TMF fiber for different coupler widths (w_g = 10 μm and w_g = 14 μm), fiber-to-coupler misalignment (x = 0 μm and x = 4 μm) and exciting fiber mode (LP_{01}, LP_{11}).

Figure 8 shows the optical intensity profiles at the grating coupler output (at a Δz = 15 μm distance from the end of the grating coupler) when the coupler is excited from a TMF fiber with just one mode with the proper polarization and azimuthal orientation. These plots are presented for the most sensitive design and the selected width from Fig. 7, that is, w_g = 10 μm (a-d) and w_g = 14 μm (e-h) waveguide widths. Two positions for the fiber are shown in the figure, centered (x = 0 μm) and with a 4 μm lateral misalignment. The field intensity is represented by color scale, being brown the most intense area and blue the least one.

TE_0 is symmetric at x = 0 μm and non-symmetric at x = 4 μm respect to x-y axes for both w_g = 10 μm (a-b) and w_g = 14 μm (e-f) waveguides. Without displacement, mode profiles exhibit a unique Gaussian profile whereas for a 4 μm displacement, a fraction of the TE_0 power is converted into TE_1 mode. That trend is more pronounced as we increase the waveguide width. Apart from that, for w_g = 14 μm, the mode profile is more confined than for

Optics EXPRESS

the other width at x = 0 μm and less confined at x = 4 μm, which is consistent with the coupling efficiency results.

TE_1 is symmetric at x = 0 μm and breaks the symmetry at x = 4 μm respect to x-y axes for both 10 μm (c-d) and 14 μm (g-h) waveguides. Undesired mode conversion is evidenced for a 4 μm displacement by the conversion of TE_1 mode into TE_0. This effect is enhanced for the w_g = 10 μm waveguide in which case most of the power has been transformed into TE_0 mode (Fig. 8(d)). LP_{11} is coupled to the TE_1 mode for both waveguide widths, nonetheless, the original mode profile is better preserved for the w_g = 14 μm waveguide.

4. Experimental results

The grating couplers with 12 μm and 14 μm waveguide widths have been fabricated on samples from 6" SOI wafers. The wafers were purchased from SOITEC and have a 220 nm thin silicon top layer and a 2 μm thick buried oxide layer. The total wafer thickness is approximately 750 μm, taking into account the silicon bulk. The NTC laboratory employed the SOI CMOS-compatible process based on an electron beam direct writing lithography on HSQ resist, followed by dry etching of 220 nm SOI wafers, a typical process to be found in fabrication foundries.

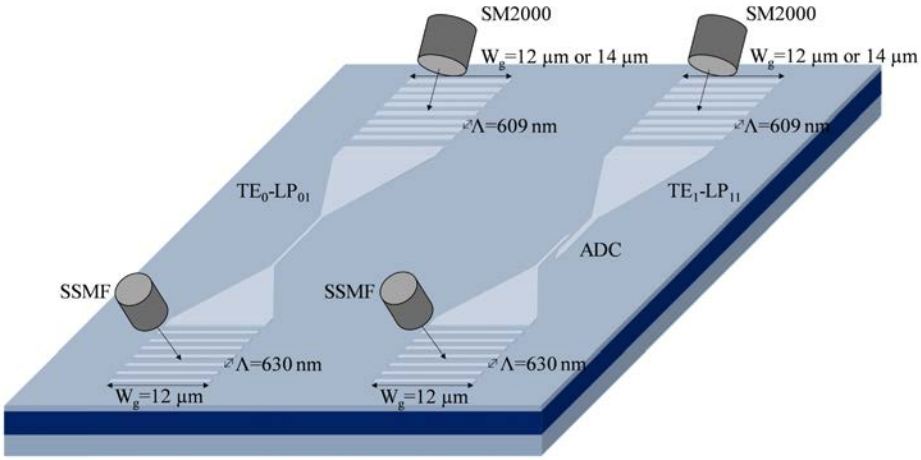

Fig. 9. 3D-sketch of the experimental configuration in order to achieve the LP_{01} and LP_{11} modes in the TMF.

Figure 9 shows the experimental configuration based on two schemes, one for the TE_0-LP_{01} mode coupling and the other for the TE_1-LP_{11}. In both cases, light is launched to a standard LP_{01}-TE_0 grating (w_g = 12 μm) by means of a standard single mode fiber (SSMF). Previously, a polarization controller is employed to adjust and maximize the coupling to the grating coupler. When the first scheme is considered, the configuration does not need an ADC as only TE_0 mode is propagated and coupled to the LP_{01} mode in the TMF. The second scheme uses a mode converter based on an asymmetrical directional coupler (ADC) in order to transform the TE_0 into TE_1 [6]. Next, the TE_1 mode reaches the output grating coupler and it is finally coupled to the TMF. The optical modes are propagated in the TMF pigtail with a length of 2 meters. Additionally, to avoid any undesirable reflection, the ADC waveguides were tapered.

In order to characterize the performance of the grating couplers (w_g = 12 μm and w_g = 14 μm wide) the insertion losses and the modal purity of the LP_{01} and LP_{11} modes in the TMF output were measured for all four cases. The modal purity has been determined by means of the normalized mode overlap integral of the measured mode with the theoretical pure LP_{01} or LP_{11} mode for the SM2000 fiber.

Optics EXPRESS

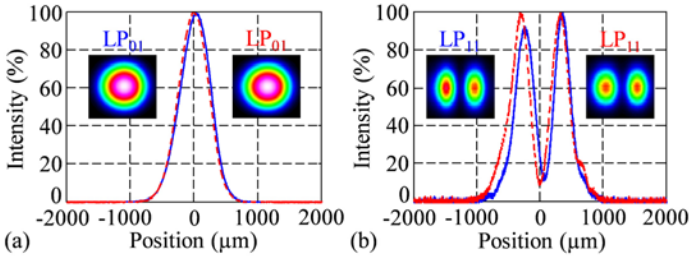

Fig. 10. Experimental intensity pattern and modal profile at the TMF from 12 μm (solid blue line) and 14 μm (dashed red line) waveguide widths for: (a) LP_{01} mode and (b) LP_{11} mode.

Figure 10 depicts the intensity pattern and modal profile of the LP_{01} and LP_{11} modes when the grating coupler is driven by the TE_0 or the TE_1 modes to be coupled to the SM2000 TMF. A CCD camera Beam Profiler (Thorlabs BP209-IR) is placed at the output of the TMF verifying the correct coupling of both modes for the 12 μm and 14 μm widths. Both LP_{01} modes achieved a perfect Gaussian profile (modal purity of 100%) and the two LP_{11} modes obtained a modal purity of 89% for the w_g = 12 μm width and 92% for the w_g = 14 μm width, respectively. The insertion losses (IL) for the LP_{01} mode were 9 dB and 8.2 dB, respectively. In the case of the LP_{11} mode, the IL obtained were 18 dB and 16 dB, respectively. It can be stated that the LP_{01} mode achieved a better power coupling than LP_{11} mode due to the extra losses added by the mode integrated mode converter needed to obtain the TE_1 mode in the experimental setup. These insertion losses values correspond to the losses from the laser output to the TMF output including all fiber pigtails, connectors and polarization controller needed for the experiment. Finally, both modes obtained an excellent modal purity and the insertion losses are lower than the state-of-the-art result for TE_1-LP_{11} vertical grating couplers in SOI technology which show insertion losses higher than 20 dB [21–23].

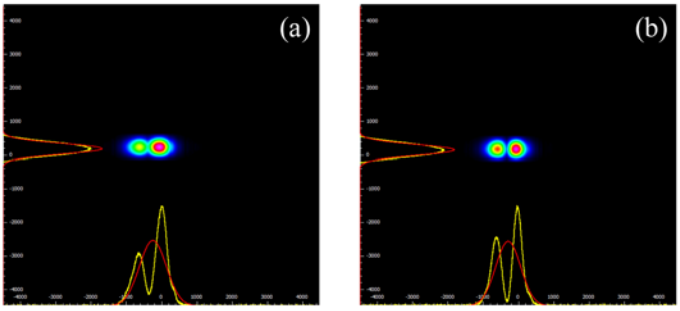

Fig. 11. Captured image of the intensity pattern and modal profile of the LP_{11} modes when a little misalignment in the coupling from fiber to grating coupler is produced for: (a) 12 μm width and (b) 14 μm width.

In order to check the sensitivity of both designs to the fiber to grating coupler misalignment, the fiber was slightly laterally misplaced when the TE_1 to LP_{11} was under measurement and the results are shown in Fig. 11. The pictures were captured moving the positioner (NEWPORT M-562 XYZ with DM-13 micrometers) around 3 μm respect to the waveguide center. Thus, the LP_{11} mode profile at the SM2000 fiber output for the w_g = 14 μm coupler obtains a higher purity (86%) than the LP_{11} mode for the w_g = 12 μm coupler (77%), as shown in Fig. 11. The experimental results confirm the greater tolerance to fiber-coupler lateral misalignments for the w_g = 14 μm design.

Optics EXPRESS

5. Conclusion

In this paper, we have reported the simulation and experimental analysis of the LP_{01} and LP_{11} fiber modes coupling to the TE_0 and TE_1 SOI waveguide modes through grating couplers. Different grating coupler widths (10 µm to 15 µm) have been assessed in terms of LP_{01}-TE_0 and LP_{11}-TE_1 coupling efficiency, sensitivity to lateral misalignment between the coupler and the fiber and design compactness. The optimum design (Λ = 609 nm, e_d = 70 nm, ff = 0.5) obtained a 49% LP_{01}-TE_0 efficiency with a 5 µm alignment tolerance whereas the LP_{11}-TE_1 efficiency is 45% with a 2.6 µm alignment tolerance. Both efficiency results are quite close to the theoretical maximum efficiency of 50%. The coupling efficiency and the sensitivity to lateral misalignment have been experimentally assessed for two different widths, 14 µm as optimum design and 12 µm as the typical width for single-mode TE_0-LP_{01} couplers. The near-field pattern at the two-mode fiber output confirms the perfect coupling of both modes for the 14 µm width with a modal purity of 100% and 90%, respectively.

Funding

Ministerio de Economía y Competitividad (MINECO/FEDER) (TEC2015-70858-C2-1-R, RTC-2014-2232-3)